

ADAPTIVE ADMITTANCE CONTROL: An Approach to Explicit Force Control in Compliant Motion

Homayoun Seraji
Jet Propulsion Laboratory
California Institute of Technology
Pasadena, CA 91109

Abstract

This paper addresses the problem of controlling a manipulator in compliant motion while in contact with an environment having an unknown stiffness. Admittance control is used as an *explicit* force control scheme in which a force setpoint is specified and is tracked by the force compensator. Two adaptive PID and PI force compensators are proposed. The compensators ensure robust tracking of step force setpoints and rejection of constant disturbances. Since the environmental stiffness can typically vary by several orders of magnitude, compensator adaptation is used to ensure a stable and uniform system performance. Dynamic simulation results for a 7 DOF Robotics Research arm are presented to demonstrate the efficacy of the proposed admittance control scheme in executing contact tasks.¹

1 Introduction

Robust and reliable operation of manipulators in contact with objects in their environment is the basic requirement for successful execution of many robotic tasks. Stable control of robot-environment interaction *poses a* technically challenging problem, and has attracted the attention of several roboticists for almost two decades [see, e.g., 1-3]. In particular, compliant motion control, which is in essence position-based force control, has been suggested by Kazerooni [4] and Lawrence [5].

The objective of this paper is to develop a simple and pragmatic approach to contact force control using the compliant motion framework. The proposed approach, called *adaptive admittance control*, is an *explicit*

force control scheme which ensures robust force setpoint tracking with desirable dynamic response. This approach is based on the concept of mechanical admittance, which relates the contact force to the resulting velocity perturbation. The adaptation of the admittance controller provides improved performance under gross variation of the environmental stiffness.

The paper is structured as follows. Section 2 discusses explicit force control within the compliant motion framework. Two adaptive admittance control schemes resulting in PII) and PI force compensators are discussed in Section 3 to ensure force setpoint tracking. In Section 4, the Robotics Research arm is used in a series of dynamic simulations to demonstrate force control. The paper is concluded in Section 5 with a review and general discussions.

2 Explicit Force Control in Compliant Motion

The underlying concept of compliant motion control is to take a position-controlled robot as a baseline system and to make the necessary modifications to this system to enable execution of constrained tasks that require robot interaction with the environment. Figure 1 shows the block diagram of a position-based explicit force control system, including the reference position X_r and the force setpoint F_r , when the robot interacts with the environment. The contact force F is fed back to the force compensator $K(s)$ which produces the position perturbation X_f , so that the end-effector tracks the modified commanded trajectory $X_c = X_r + X_f$.

Now, since the manipulator position control system ensures Cartesian trajectory tracking, the internal position controller, in effect, decouples the robot dynamics, and we can replace the end-effector position vector X in the control diagram by the scalar x , which can represent

¹ The research described in this paper was carried out at the Jet Propulsion Laboratory, California Institute of Technology, under contract with the National Aeronautics and Space Administration.

any element of X . Furthermore, following Kazerooni [4], Lawrence [5], and other researchers, it is reasonable to model each position-controlled end-effector coordinate by a second-order linear continuous-time system, so that for each end-effector coordinate the scalar transfer-function relating the commanded position x_c to the actual position x is given by

$$G(s) = \frac{x(s)}{x_c(s)} = \frac{K_m}{J_m s^2 + B_m s + K_m} = \frac{b}{s^2 + as + b} \quad (1)$$

where J_m , B_m , and K_m are the position-controlled manipulator mass, damping and stiffness parameters in Cartesian-space respectively, $a = \frac{B_m}{J_m}$ and $b = \frac{K_m}{J_m}$. This simple model can adequately account for the small time-delays involved in the forward and inverse kinematic calculations as well as the dynamics of the position-controlled joint servo loops. This model is particularly suitable for industrial robots that use high gear ratios which attenuate the nonlinear manipulator dynamics and make the second-order joint motor dynamics dominant.

The environment can often be modeled as a linear spring with coefficient of stiffness K_{en} along the Cartesian axis of interest. Therefore, the force-displacement model for the environment is given by Hooke's law as

$$F = K_{en}(x - x_e) \quad (2)$$

where x_e is the nominal position of the environment. Similarly, the force/torque sensor mounted on the end-effector can be modeled as a pure spring with the stiffness coefficient K_{sn} , since the dynamics of the sensor can be neglected in comparison with the compensator and manipulator time-constants. Therefore, the effective stiffness of the sensor plus the environment in a Cartesian direction is given by $K_e = (1/K_{en} + 1/K_{sn})^{-1}$. Note that although the manipulator-environment interaction can be modeled in detail as a high-order dynamical system, the stiffness is often the dominating factor in contact tasks such as assembly, mating, and deburring [5, 6, 7]. Furthermore, this simple model is mathematically tractable and has been widely adopted by several researchers. Note that during contact with the environment, the dynamic model of the position-controlled end-effector coordinate is modified by the environment due to natural force feedback as

$$\bar{G}(s) = \frac{x(s)}{x_c(s)} = \frac{b}{s^2 + as + b'} \quad (3)$$

where $b' = \frac{(K_m + K_e)}{J_m}$.

In the next section, we develop two force compensators based on admittance control to accomplish force setpoint tracking.

3 Adaptive Admittance Control

In contrast to pure position control which rejects disturbance forces in order to track a given reference motion trajectory, the force compensator $K(s)$ attempts to comply with the environmental interaction and react quickly to contact forces by rapidly modifying the reference motion trajectory. A proper measure of effectiveness of the compliant, motion control is the *mechanical admittance* Y defined as [8]

$$Y = \frac{v_f}{F} \quad (4)$$

where v_f is the end-effector velocity and F is the contact force, both at the point of interaction. A large admittance corresponds to a rapid motion induced by applied forces; while a small admittance represents a slow reaction to contact forces. Based on the above discussions, the force compensator transfer-function $K(s) = \frac{x_f(s)}{e(s)}$ is expressed as the product

$$K(s) = \frac{1}{s} \cdot Y(s) \quad (5)$$

where the admittance $Y(s)$ relates the force error $e = F_r - F$ to the end-effector velocity perturbation $v_f(s)$; i.e., $Y(s) = \frac{v_f(s)}{e(s)}$. For a known environmental stiffness, an admittance $Y(s)$ can be constructed to achieve a desirable force response with small or zero error, low overshoot, and rapid rise time. However, the same admittance typically exhibits sluggish response in contact with softer environments, and goes unstable when contacting stiffer environments. In other words, because different environments have diverse stiffness which can vary over several orders of magnitude, a fixed admittance design based on a nominal environment leads to non-uniform dynamic performance and often instability. To overcome this problem, we propose *adaptive admittance control* where the parameters of the admittance $Y(s)$ are tuned automatically on-line based on the force tracking performance of the system. This approach provides stable uniform performance under gross variations in the environmental stiffness.

In this section, we consider two classes of adaptive admittances that can be used for force control within the compliant motion control framework. The second-order admittance leads to an adaptive PID force compensator, while the first-order admittance leads to an adaptive PI force compensator.

3.1 Adaptive PID Force Compensator

In this section, an adaptive second-order admittance control scheme will be developed to accomplish force control within the compliant motion framework.

Consider the admittance-based compliant control system shown in Figure 1. Let us choose a second-order admittance model as

$$Y(s) = k_d s^2 + k_p s + k_i \quad (6)$$

resulting in the PID force compensator

$$K(s) = \frac{1}{s} \cdot Y(s) = k_d s + k_p + \frac{k_i}{s} \quad (7)$$

where $\{k_p, k_i, k_d\}$ are the proportional, integral, and derivative force feedback gains, respectively. This leads to the force feedback law

$$x_f = k_d \frac{d}{dt} e + k_p e + k_i \int_0^t e dt \quad (8)$$

For the purpose of control law development, we consider the control signal x_f to be comprised of proportional and derivative terms in $\{e, \dot{e}\}$ together with an auxiliary signal $g(t)$ which contains the integral term, that is

$$x_f(t) = g(t) + k_p(t)e(t) + k_d(t)\dot{e}(t) \quad (9)$$

where $\{k_p(t), k_d(t)\}$ are the adaptive proportional and derivative force feedback gains, respectively. On applying the control law (9) to the system shown in Figure 1, and noting that F_r, k_e , and x_e are constant, we obtain the force error dynamics as

$$\ddot{e} + [a + b k_e k_d] \dot{e} + [b' + b k_e k_p] e = b' [F_r - F_x] - b k_e g \quad (10)$$

where $F_x = k_e [\frac{b}{b'} x_r - x_e]$ is the steady-state contact force due to constant x_r with no force feedback ($x_f = 0$). Equation (10) represents the “adjustable system” in the model-reference adaptive control (MRAC) framework. Suppose that the *desired* behavior of the force tracking-error e_m is specified as

$$\ddot{e}_m + 2\zeta\omega\dot{e}_m + \omega^2 e_m = 0 \quad (11)$$

where ζ and ω are the user-specified damping ratio and unclamped natural frequency of the force error dynamics. Equation (11) constitutes the “reference model” within the MRAC framework. Following [9], the adaptation laws for $\{g(t), k_p(t), k_d(t)\}$ which ensure that the solution $e(t)$ of the error dynamics (10) tends asymptotically to the solution $e_m(t)$ of the reference model (11) are given by

$$\begin{aligned} \dot{g}(t) &= w_p e(t) + w_d \dot{e}(t) \\ g(t) &= g(0) + \alpha_1 \int_0^t q(t) dt + \alpha_2 q(t) \\ k_p(t) &= k_p(0) + \beta_1 \int_0^t q(t) e(t) dt + \beta_2 q(t) e(t) \end{aligned} \quad (12)$$

$$k_d(t) = k_d(0) + \gamma_1 \int_0^t q(t) \dot{e}(t) dt + \gamma_2 q(t) \dot{e}(t)$$

where (w_p, w_d) are the positive position and velocity weighting factors, $(\alpha_1, \alpha_2, \gamma_1)$ are the positive integral adaptation gains, $(\beta_1, \beta_2, \gamma_2)$ are the positive or zero proportional adaptation gains, and $[g(0), k_p(0), k_d(0)]$ are the positive initial values chosen to provide appropriate initial position perturbation signal and initial proportional and derivative gains for the control system. The force control scheme is shown in Figure 2. Using (12), the force control law (9) can be written as

$$x_f(t) = x_f(0) + k_p^*(t)e(t) + k_i^* \int_0^t e(t) dt + k_d^*(t)\dot{e}(t) \quad (13)$$

Where $k_p^*(t) = \alpha_1 w_d + \alpha_2 w_p + k_p(t)$ is the adaptive proportional gain, $k_i^* = \alpha_1 w_p$ is the constant integral gain, and $k_d^*(t) = \alpha_2 w_d + k_d(t)$ is the adaptive derivative gain and $x_f(0) = g(0)$. It is seen that the position perturbation $x_f(t)$ due to contact force is generated by a PID controller driven by the force tracking-error $e(t)$, where the controller is composed of a constant-gain PID term and an adaptive-gain PD term.

From a practical point of view, the contact force F measured by the force/torque sensor is often a noisy signal and hence direct differentiation of this signal to obtain \dot{e} is undesirable. To overcome this problem, \dot{e} is replaced by $-k_e \dot{x}$, as suggested by $F = k_e(x - x_e)$, where F_r is constant. Furthermore, to ensure robustness in the presence of the unmodeled environmental dynamics, we slightly modify the adaptation laws (12) using the a-modification terms [10]. Thus, the modified adaptation laws using the velocity signal \dot{x} are given by

$$\begin{aligned} x_f(t) &= g(t) + k_p(t)e(t) - k_v(t)\dot{x}(t) \\ g(t) &= g(0) + \alpha_1 \int_0^t q(t) dt + \alpha_2 q(t) - \sigma_1 \int_0^t g(t) dt \\ k_p(t) &= k_p(0) + \beta_1 \int_0^t q(t) e(t) dt + \beta_2 q(t) e(t) - \sigma_2 \int_0^t k_p(t) dt \\ k_v(t) &= k_v(0) - \lambda_1 \int_0^t q(t) \dot{x}(t) dt - \lambda_2 q(t) \dot{x}(t) - \sigma_3 \int_0^t k_v(t) dt \end{aligned} \quad (14)$$

$$\dot{q}(t) = w_p e(t) - w_v \dot{x}(t)$$

where $\lambda_1 = \gamma_1 k_e$, $\lambda_2 = \gamma_2 k_e$, $w_v = w_d k_e$ and $\sigma_1, \sigma_2, \sigma_3$ are small positive constants. The addition of the a-modification terms enhances robustness in the presence of the unmodeled dynamics, at the price of a residual force tracking-error of Order (o^*),

3.2 Adaptive PI Force Compensator

In this section, an adaptive first-order admittance control scheme will be developed for force control within the compliant motion framework.

Consider the admittance-based compliant control system shown in Figure 1, with the first-order admittance model

$$Y(s) = k_p s + k_i \quad (15)$$

resulting in the PI force compensator

$$K(s) = \frac{1}{s} \cdot Y(s) = k_p + \frac{k_i}{s} \quad (16)$$

and the force feedback law

$$x_f = k_p e + k_i \int_0^t e dt \quad (17)$$

where $\{k_p, k_i\}$ are the proportional and integral force feedback gains, respectively. In comparison with the second-order admittance model (6) used in Section 3.1, the first-order admittance model (15) has the advantage of *not* requiring the rate-of-change of the force error e , which is a noisy signal. As a result, the PI control scheme is much simpler to implement in practice. However, the price paid for this simplicity is that there are now insufficient adjustable gains in the compensator to ensure that the error dynamics (10) follows an arbitrary user-specified reference model (11). In this case, the force feedback gains are chosen to ensure merely that the error dynamics is asymptotically stable, so that $e(t) \rightarrow 0$ as $t \rightarrow \infty$.

Applying the PI control law (17) to the system shown in Figure 1, we obtain the dynamic model of the force tracking-error as

$$\ddot{e} + a\dot{e} + [b' + bk_e k_p]e + bk_e k_i \int_0^t e dt = b'[F_r - F_x] \quad (18)$$

It is seen that the coefficient of \ddot{e} in the error dynamics (18) is constant and can not be affected by the controller gains $\{k_p, k_i\}$. This is expected since the force compensator does not have any active damping term $k_d \dot{e}$ to contribute to the passive damping "a" of the system. Now, we need to find the adaptation laws for the proportional gain $k_p(t)$ and the integral gain $k_i(t)$ to ensure that (18) represents an asymptotically stable system.

To simplify the stability analysis, we choose the integral gain k_i as a constant and employ an adaptation law for the proportional gain k_p as a nonlinear function of the force tracking-error e . We adopt the Lyapunov approach to investigate the stability of the third-order nonlinear error differential equation (18). For a class of third-order nonlinear differential equations such as

(18), Barbashin [11] has obtained specific stability criteria using a Lyapunov analysis. Applying Barbashin's method to the error dynamics (18) yields the following three stability conditions:

- (i) $a > 0$
- (ii) $b k_e k_i [\int_0^t e dt]^2 > 0 \rightarrow k_i > 0$ (19)
- (iii) $a[b' + b k_e k_p] - b k_e k_i > 0 \rightarrow k_i < a \left[k_p + \frac{b'}{b k_e} \right]$

Thus, we conclude that the stability of the nonlinear differential equation (18) is guaranteed provided that

$$0 < k_i < a \left[k_p + \frac{b'}{b k_e} \right] \quad (20)$$

Note that conservative estimates of the attenuation factor a and the forward path gain $\frac{b k_e}{b'}$ can readily be obtained from the open-loop response of the contact force F to the step reference position x_r with no force feedback ($x_f = 0$). Furthermore, observe that closed-loop stability is attained for *all* environmental stiffness k_e provided that the following relationship holds between the proportional and integral gains

$$0 < k_i < a k_p \quad (21)$$

It is seen that the stability condition (21) does not contain the stiffness of the environment k_e . One viable choice for the proportional gain k_p as a function of the force tracking-error e is given by

$$k_p(t) = k_{p0} + \alpha e^2(t) \quad (22)$$

where k_{p0} is the positive constant value chosen for k_p when $e = 0$, and α is the positive constant adaptation gain chosen by the user to reflect the sensitivity of k_p to e . Notice that the adaptive term αe^2 contributes only to the transient response by increasing the proportional gain k_p so as to reduce the tracking-error e . When e is small, the effect of αe^2 is diminished and k_p restores to its initial value k_{p0} . From (20) and (22), provided that the controller gains are chosen such that

$$0 < k_i < a \left[k_{p0} + \frac{b'}{b k_e} \right] \quad (23)$$

the stability of the closed-loop compliant control system is guaranteed. Figure 3 shows a block diagram of the adaptive PI force control scheme.

Equation (22) implies that

$$\dot{k}_p(t) = 2\alpha e(t)\dot{e}(t) \quad (24)$$

When e and \dot{e} have the same sign, the force response has an *unfavorable trend* since the force error is negative (or

positive) and is decreasing further (increasing further). In these cases, $e\dot{e} > 0$ and from (24), $k_p > 0$, and the controller gain k_p increases. When e and \dot{e} have opposite signs, the force response has a *favorable trend* since the force error is positive (or negative) and is decreasing (or increasing) toward zero. In these cases, $e\dot{e} < 0$ and $k_p < 0$ which means that k_p will decrease. We conclude that when the force response has an unfavorable trend, the proportional gain increases rapidly to correct the response; whereas during a favorable trend, the gain decreases since no corrective action is called for. Notice that the proportional gain will adjust continuously until the steady-state is reached when $e = \dot{e} = 0$ and k_p assumes the specified constant value k_{p0} .

4 Simulation Study

The force control scheme described in Section 3 is now applied through computer simulations to the 7 DOF Robotics Research Corporation (RRC) Model K-1607 arm, shown in Figure 4. The full nonlinear dynamic model for this arm is integrated into a graphics-based robot simulation environment hosted on a Silicon Graphics Personal IRIS workstation [12]. In the simulation, the robot position control system employs a high-performance adaptive controller described in [13]. **This controller ensures that any commanded end-effector position trajectory x_c is tracked accurately.**

The simulation study demonstrates the capability of the proposed admittance control scheme to achieve a desired end-effector/environment contact force. In this study, a frictionless reaction surface modeled as linearly elastic with a stiffness of 100 lb./in in series with a damper having the friction coefficient of 10 lb.sec./in is placed in the robot workspace. This reaction surface is oriented normal to the y axis and is located at $y_c = -22.125$; thus the measured contact force F is modeled as

$$F = \begin{cases} 0 & \text{if } y \leq -22.125 \\ 100(y + 22.125) + 10\dot{y} & \text{if } y > -22.125 \end{cases}$$

The task requires the exertion of a 10 lb contact force normal to the reaction surface while tracking a smooth 5 in trajectory tangent to the surface. Thus we define $F_r = 10$ and $x_r = x_i + 2.5[1 - \cos(\pi/5)t]$ for $t \in [0, 5]$, where x_i is the x component of the initial end-effector position. For simplicity, the end-effector orientation and z coordinate are maintained at their initial values throughout the task.

To illustrate robustness of the force control scheme in accommodating unexpected changes in the environmental stiffness, the stiffness k_e is changed abruptly from $k_e = 100$ lb/in to $k_e = 25$ lb/in at the midpoint

of the x_r trajectory at $t = 2.5$ seconds. The control objective is to maintain the contact force at 10 lb despite this stiffness variation. This situation can occur in practice when tracking along a surface composed of two materials with different stiffnesses.

Let us apply the adaptive PI force control law

$$y_f(t) = [k_{p0} + \alpha e^2(t)]e(t) + k_i \int_0^t e(t)dt \quad (25)$$

developed in Section 3.2, where $e = F_r - F$ is the force tracking-error. This control scheme has the attractive feature of *not* requiring force rate information for implementation. The desired force setpoint is specified as

$$F_r(t) = \begin{cases} 5[1 - \cos \pi t] & t < 1 \\ 10 & t \geq 1 \end{cases}$$

so that the force setpoint rises smoothly to 10 lb in 1 second.

First, the open-loop response of the contact force F to the step reference input y_r with no force feedback ($y_i = 0$) is obtained. The response indicates that the robot-plus-position controller-plus-reaction surface can be approximated by a linear second-order transfer function with the forward path gain $\frac{b k_e}{b^2} = 100$ and the attenuation factor $a = 10$, since for the command $y_r = 0.2$ inches the force response reaches the steady-state value $F_{ss} = 20$ lb in 1 second. Following Section 3.2, the integral gain k_i and the initial proportional gain k_{p0} are chosen as $k_i = 0.10$ and $k_{p0} = 0.004$ to satisfy the inequality $0 < k_i < a \left[\frac{k_{p0}}{b k_e} \right] \frac{b c}{b k_e}$. The rate-of-adaptation of the proportional gain is chosen as $\alpha = 0.0001$ and the reference position is set to $y_r = 0.2$ inches. Figures 5a and 5b show the variations of the contact force F and the adaptive proportional gain k_p during the task. From Figure 5a, it is seen that F tracks the desired force setpoint F_r in the steady-state, which is reached in 1 second. The contact force is then perturbed at $t = 2.5$ seconds due to the change in environmental stiffness, but recovers subsequently due to the integral action to settle again at the desired setpoint $F_r = 10$ lb in the steady-state. Figure 5b shows that the adaptive term $\alpha e^2(t)$ in the proportional gain k_p causes an increase in the value of k_p during the transient responses, where there are discrepancies between the actual and desired forces. Once the force tracking-error e diminishes to zero in the steady-state, the proportional gain returns to its initial value k_{p0} . Hence, the compensator adaptation improves the transient behavior by increasing k_p automatically when e is large, without affecting the steady-state performance.

5 Conclusions

Force control based on compliant motion is discussed in this paper. The admittance control approach is an explicit force control scheme that uses force setpoint as command and accomplishes contact force control directly. The adaptive compensator gains ensure stable and uniform performance in contact with environments having unknown stiffnesses.

It can readily be shown that when the constant force setpoint F_r and the step force disturbance F_d are applied to the system, the contact force F tracks the force setpoint F_r and rejects the force disturbance F_d when the steady-state is reached. Furthermore, when the system parameters $\{a, b, b', k_e\}$ or the compensator gains $\{k_p, k_i, k_d\}$ undergo gross and arbitrary variations, the control system is *robust* in the sense that the setpoint regulation and disturbance rejection characteristics are retained, *provided that the closed-loop system remains stable*.

We conclude that the adaptive admittance control schemes developed in this paper for generating the position perturbation are extremely simple and computationally very efficient. As a result, the control schemes can be implemented for real-time force control with a high sampling rate, which is critical for closed-loop stability of force control loops that contain typically large environmental stiffness k_e . Furthermore, since the controller terms do not require knowledge of x_e and \dot{x}_e and are adjusted on-line based on the force tracking performance through e and \dot{e} , the controller can rapidly adapt itself to gross changes in the environmental parameters x_e and k_e as demonstrated in Section 4.

References

- [1] D. E. Whitney: "Force Feedback Control of Manipulator Fine Motions," ASME Journal of Dynamic Systems, Measurement, and Control, pp. 91-97, 1977.
- [2] M. Raibert and J. Craig: "Hybrid Position/Force Control of Manipulators", ASME Journal of Dynamic Systems, Measurement, and Control, Vol. 102, No. 2, pp. 126-133, 1981.
- [3] N. Hogan: "Impedance Control: An Approach to Manipulation, Parts I-III", ASME Journal of Dynamic Systems, Measurement, and Control, Vol. 107, No. 1, pp. 1-24, 1985.
- [4] H. Kazerooni, B. J. Waibel, and S. Kim: "On the Stability of Robot Compliant Motion Control," ASME Journal of Dynamic Systems, Measurement, and Control, Vol. 112, pp. 417-426, 1990.
- [5] D. A. Lawrence and R. M. Stoughton: "Position-Based Impedance Control: Achieving Stability in Practice," Proc. AIAA Guidance, Navigation, and Control Conference, pp. 221-226, Monterey, 1987.
- [6] H. Ishikawa, C. Sawada, K. Kawase, and M. Takata: "Stable Compliance Control and its Implementation for a 6 DOF Manipulator," Proc. IEEE International Conference on Robotics and Automation, pp. 98-103, Scottsdale, 1989.
- [7] O. Khatib and J. Burdick: "Motion and Force Control of Robot Manipulators," Proc. IEEE International Conference on Robotics and Automation, Vol. 3, pp. 1381-1386, San Francisco, 1986.
- [8] W. S. Newman: "Stability and Performance Limits of Interaction Controllers," ASME Journal of Dynamic System., Measurement, and Control, Vol. 114, pp. 563-570, 1992.
- [9] H. Seraji: "Decentralized Adaptive Control of Manipulators: Theory, Simulation and Experimentation," IEEE Transactions on Robotics and Automation, Vol. 5, No. 2, pp. 183-201, 1989.
- [10] P. A. Ioannou and P. V. Kokotovic: *Adaptive Systems with Reduced Models*, Springer-Verlag, New York, 1983.
- [11] W. J. Cunningham: "An Introduction to Lyapunov's Second Method," in 'Work Sessions in Lyapunov's Second Method,' L. F. Kazda (Ed.), 1960.
- [12] K. Glass and R. Colbaugh, "A Computer Simulation Environment for Manipulator Controller Development," NMSU Internal Publication, 1992.
- [13] R. Colbaugh, H. Seraji, and K. Glass: "Direct Adaptive Impedance Control of Robot Manipulators," Journal of Robotic Systems, Vol. 10, No. 2, pp. 217-224, 1993.

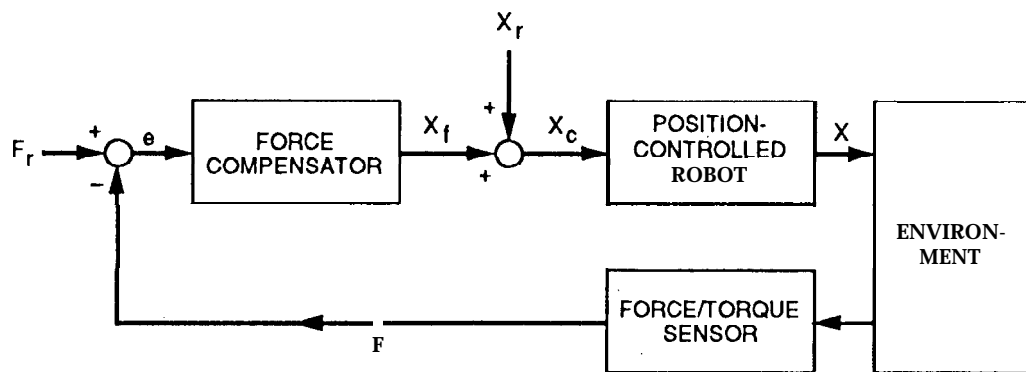


Figure 1. Position-based explicit force control system

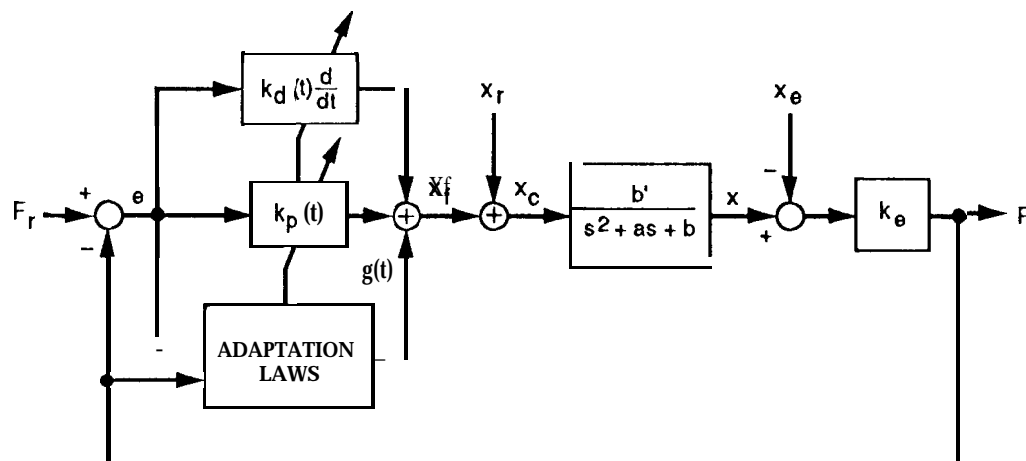


Figure 2. Adaptive PID force control scheme

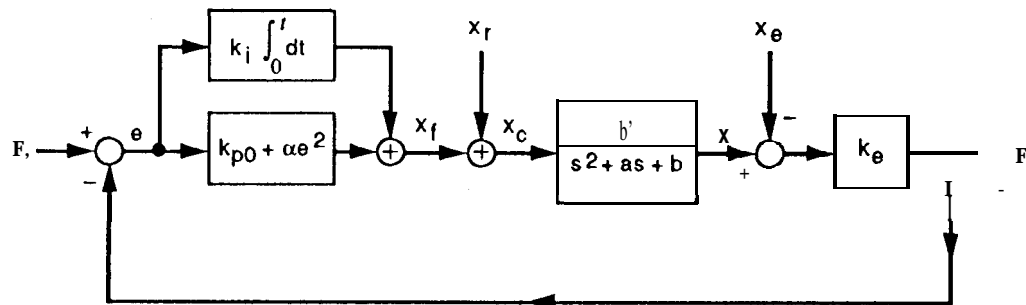


Figure 3. Adaptive Pi force control scheme

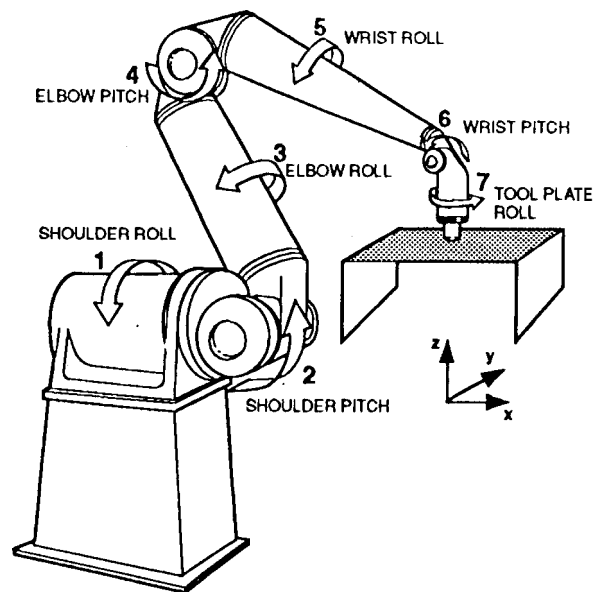


Figure 4, Robotics Research arm In contact with a surface

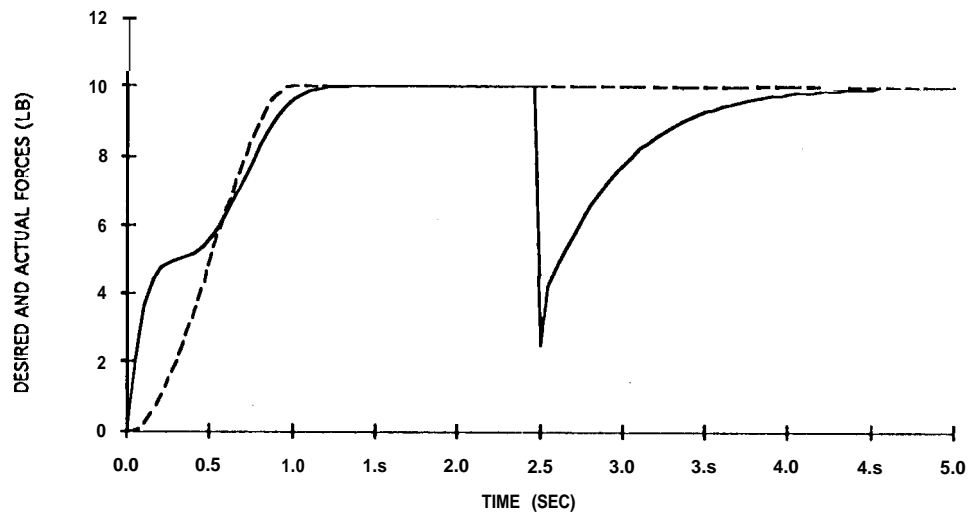


Figure 5a. Variation of the contact force F in the simulation study

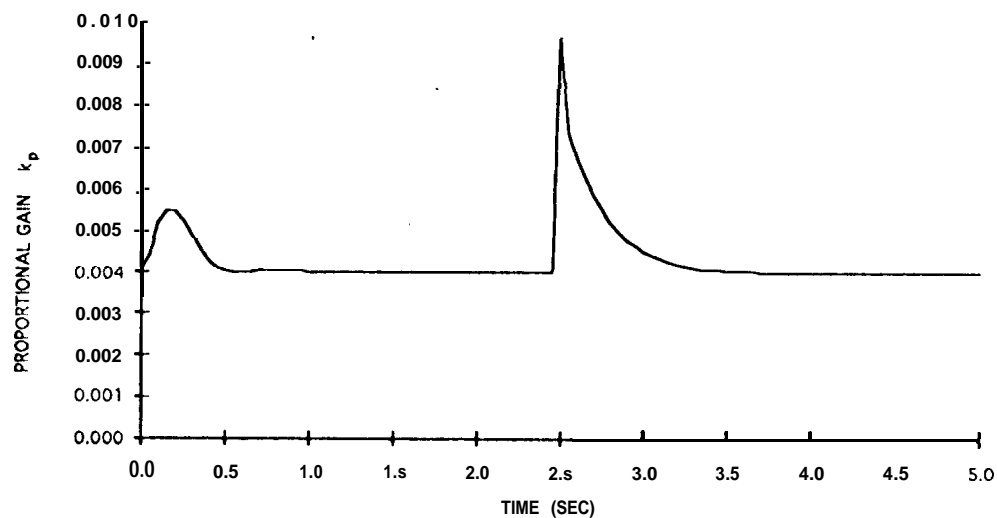


Figure 5b. Variation of the adaptive proportional gain k_p in the simulation study